Vietnam Journal of Science and Technology ***62*** *(4) (2024) 713-724*

doi:10.15625/2525-2518/17206

Fabrication of alpha-tocopheryl acetate-loaded nanoemulsion towards cosmetic application

Khanh Hoang Vuong[1], Tuong Van Vo Le[1], Doan Tran Buu Tai[1], Tan Phuoc Ton[1], Dang Le Hang[1], Nguyen Dinh Trung[1], Ngoc Quyen Tran[1, 2, *]

[1]*Institute of Applied Materials Science, Vietnam Academy of Science and Technology, Ho Chi Minh city, Viet Nam; 1B TL 29, Thanh Loc District 12, HCMC, Viet Nam*

[2]*Graduate University of Science and Technology, Vietnam Academy of Science and Technology, Ho Chi Minh city, Viet Nam 1B TL 29, Thanh Loc Ward, District 12, HCMC, Viet Nam*

[*]Email: *tnquyen@iams.vast.vn*

Received: 7 June 2022; Accepted for publication: 28 March 2023

Abstract. Recently, fabrication of nanoemulsion has drawn substantial interest in the field of pharmaceutical chemistry, particularly the development of nanosystems for the delivery of bioactive compounds. The idea of this material is to encapsulate and carry water-insoluble active agents to the targeted site. Our work focuses on the ideal delivery system for alpha-tocopheryl acetate (AVE), which currently covers a broad range of medications, supplementation and cosmetics. To put it in detail, we investigated different kinds of pluronic emulsifiers (pluronic F127, pluronic P123 and their mixture) to fabricate the AVE-loaded nanoemulsion particles. The structure, physicochemical properties, stability and biocompatibility of various formulations were compared using Fourier-transform infrared spectroscopy (FT-IR) spectra; Dynamic light scattering (DLS); macroscopic and microscopic images; Transmision electron microscopy (TEM) and *in vitro* cytotoxicity test. The obtained results exhibited a high stability of AVE-loaded pluronic mixture as compared to that of the free-AVE sample. Moreover, the dual pluronic formulation also showed a great cytocompatibility which could be utilized in topical and transdermal delivery.

Keywords: alpha-tocopheryl acetate, pluronic, nanoemulsion, cosmetic.

Classification numbers: 1.3.3, 2.5.3, 2.9.4

1. INTRODUCTION

Alpha-tocopheryl acetate (AVE) is known as a fat-soluble antioxidant, found in various types of vegetable oil such as hazelnut oil; sunflower oil; wheat germ oil; canola oil; almond oil; etc. Natural AVE has eight vitamers, including: alpha; beta gamma; and delta forms for both tocopherols and tocotrienols. Although all stereoisomers are absorbed with approximately equivalent efficiencies by the intestinal lumen, alpha-tocopherol is proven to be the most active form due to the protection by alpha-tocopherol transfer protein from side-chain degradation, contributing to the maintenance of normal alpha-tocopherol concentrations [1]. For industrial

applications, both natural and synthetic AVE are converted to acetate ester forms - which are more chemically stable and have a longer shelf-life.

Apart from its general antioxidant property, different forms of AVE have drawn scientists to investigate their different anti-inflammatory, neuroprotective, pro- and anti-malignant potentials [2-4]. Although clinical evidence for treatments utilising AVE is still inconsistent [5], topical AVE has drawn an exclusive interest towards skincare applications due to its anti-oxidative and photo-protective properties. However, the nature of commercially available - synthetic AVE being its high viscousity; light-sensitivity; a skin irritant and difficult incorporation into cosmetic formulations still present limitations in AVE's potential applications [6]. These obstacles have led to the innovation of various novel formulations for dermatological use during the last decade [7]. The work of Trombino's research team focusing on stearyl ferulate-based solid lipid nanoparticles as a vehicle for both beta-carotene and alpha-tocopherol suggested a novel formulation to prevent skin damage [8]. In 2013, α-tocopherol-loaded solid lipid nanoparticle systems were optimized and characterized by Decalvarho *et al*. using a hot - high homogenization technique that possessed promising potential in the cosmetic industry [9]. These are two of the several studies indicating the potential of solid – lipid nanoparticle systems in terms of fat-soluble carriers, however, it remains to be considered due to the resultant particle size exceeding 100 nm. The physicochemical properties of solid – lipid nanoparticle systems are significantly affected by the nature and amount of added ingredients and the technique utilized. An optimal formulation is a non-irritant and stable system where skin permeation is facilitated and integrated with the lipids present in the cornified layer.

In this work, we investigated pluronic F127 and P123 for the encapsulation of lipophilic AVE and aimed to formulate a nanoemulsion system that can maximize the concentration of AVE acetate loaded. Pluronic F127 and P123 are amphiphilic emulsifiers composed of tri-block copolymers of hydrophilic poly (ethylene oxide) and hydrophobic poly (propylene oxide) [10]. According to many aforementioned promising approaches, pluronics are able to assemble into micelles in an aqueous environment and accommodate lipophilic substances in the central hydrophobic core area [10, 11]. Of particular interest is the combination of pluronic F127 and pluronic P123 with the optimal ratio of 1:1 possesses several preferred features for drug delivery applications due to the stability of the emulsified nanoparticles. Additionally, ultrasonication was investigated in our work to reduce the particle size, due to its high energy output – ideal for breaking down particle agglomerates and dispersing nano-size particles into aqueous environments. The size of nanoparticles is expected to be below 100 nm, which enables improved absorption, better texture and possible effectiveness [12, 13].

2. MATERIALS AND METHODS

2.1. Materials and sample preparation

AVE acetate (Mw: 472.8 g/mol and viscosity: 5,706 mm^2/s) was purchased from BASF (Germany) and stored at room temperature. Pluronic F127 (Mw: 12600 g/mol) and Pluronic P123 (Molecular weight: 5750 g/mol) were supplied from BASF (Germany).

The formulation of nanoemulsion was developed using the ultrasonication method as demonstrated in Fig. 1. To prepare pluronic solutions of 8 wt.%, the required amount of pluronic was weighed and added into a beaker containing cold – distilled water. The composition of each formulation was illustrated in Table 1. The mixture was stirred at the temperature under 14 ^oC for 2 hours until yielding a clear pluronic solution. Ultra sonicator (Hielscher UP200Ht) was set up with A = 65 % and C = 35 %. The ultrasonic process was carried out in a cold environment at

15 ^{o}C. The pluronic sample was ultrasonicated for 6 minutes, repeated 2 times, and the interval between each consecutive ultrasonication was 2 minutes. AVE was added drop-wise into the pluronic solution during the intervals. Finally, the mixture was ultrasonicated for another 6 minutes to form a highly transparent solution. The chemical structures of the products were verified using Fourier transform infrared spectroscopy (FT-IR, Horiba, Japan).

Table 1. AVE-loaded nanoemulsion formulations.

Formulation	Composition	Ratio (wt.%/wt.%)
F1	P123/AVE	8/8
F2	F127/AVE	8/8
F3	F127/P123/AVE	8/8/8
F4	P123/AVE	16/8
F5	F127/AVE	16/8

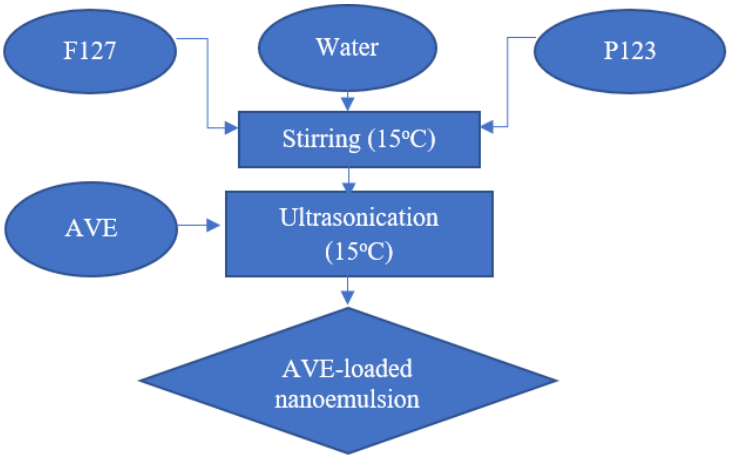

Figure 1. Schematic diagraph for AVE-loaded nanoemulsion preparation.

2.2. Dynamic light scattering (DLS) measurement

Micelle size and size distribution of AVE-loaded nanoemulsion systems were determined by SZ-100 Nanopartica Series Instrument (Horiba SZ-100) at 25 ^{o}C and 90^{o} or 173^{o} scattering angle. Each nanoemulsion sample was diluted with distilled water to the concentration of 1000 ppm and sonicated using a water bath sonicator (ELMA S 100H) prior to the examination. All measurements were conducted in a glass cuvette and used distilled water as the dispersant. The experiments were conducted at Institute of Applied Materials Science, Vietnam Academy of Science and Technology.

2.3. Transmission electron microscopy (TEM) imaging

The morphology of the nanoemulsion systems were observed with transmission electron microscope (TEM, JEM – 1400 JEOL) at 25 ^{o}C. The experiments were conducted at Ho Chi Minh City University of Technology.

2.4. Evaluation of drug loading and encapsulation efficiencies

The efficiencies of active agent (AVE) loading and subsequent encapsulation within the F127-P123 8/8 (%, w/v) nanoemulsion were evaluated utilizing UV-Vis spectrophotometry. Absorbance at wave length 205 nm was recorded for the samples [14]. The experiments were performed in triplicates, and the equations provided below were employed to approximate the drug loading (DL %) and encapsulation (EE %) efficiencies of AVE in the sample, respectively [15, 16].

$$\boldsymbol{DL}\ (\%) = \frac{(\boldsymbol{Sample\ amount\ of\ AVE})}{(\boldsymbol{Total\ amount\ of\ nanoemulsion})} \times \mathbf{100} \quad (1)$$

$$\boldsymbol{EE}\ (\%) = \frac{(\boldsymbol{Sample\ amount\ of\ AVE})}{(\boldsymbol{Total\ amount\ of\ AVE})} \times \mathbf{100} \quad (2)$$

2.5. *In vitro* study of drug release

Release behaviour of AVE from the F3 nanoemulsion was investigated via subjecting the sample to dialysis against 1 % (v/v) tween 80/phosphate buffer (pH 7.4) as medium at 37 °C in order to simulate the conditions of a physiological environment. The assessed sample was prepared by loading 2 mL of F3 nanoemulsion into dialysis bags (MWCO = 3500 Da). Subsequently, the sample bags were submerged in 20 mL of the medium and the container vials were left to stir at 37 ± 1 °C. At predetermined points in time (i.e., 1; 3; 5; 7; 9; 12 and 24 hours), 1 mL of the assessed samples was removed and replenished with the identical volume of fresh medium. Another sample set of free AVE was prepared in ethanol (8 %, w/v) then dialyzed against distilled water as medium (MWCO = 3500 Da), following the procedure above to serve as the control. The amount of AVE released present in the media was monitored by recording the absorbance at the wavelength of 205 nm with UV-Vis spectrophotometry. All experiments were performed in triplicates and the amount of AVE released was approximated with the following equation [16, 17]:

$$\boldsymbol{Q} = \boldsymbol{C_n V_s} + \boldsymbol{V_t} \sum_{i=1}^{n-1} \boldsymbol{C_{n-1}} \quad (3)$$

whereby, Q: amount of AVE released from nanoemulsion; C_n: concentration at time t; V_s: volume of medium; V_t: volume of release sample; $\sum_{i=1}^{n-1} \boldsymbol{C_{n-1}}$: concentration of AVE released as a function of time.

2.6. Release kinetics

Analysis and determination of drug release mechanism were performed by fitting the *in vitro* release data into various mathematical models with their respective equations given below [18, 19]:

$$\textit{Zero order:}\quad \boldsymbol{C} = \boldsymbol{k_0 t} \quad (4)$$

$$\textit{First order:}\quad \log \boldsymbol{C_0} - \log \boldsymbol{C_t} = \frac{\boldsymbol{k_1 t}}{\mathbf{2.303}} \quad (5)$$

$$\textit{Higuchi model:}\quad \boldsymbol{Q} = \boldsymbol{k_H t^{1/2}} \quad (6)$$

$$\textit{Korsmeyer-Peppas model:}\quad \boldsymbol{M_t} - \boldsymbol{M_\alpha} = \boldsymbol{k t^n} \quad (7)$$

whereby, C: concentration of drug; C_0: initial concentration; C_t: concentration at time t; t: time; Q: amount of drug released in time; $M_t - M_\alpha$: fraction of drug released at time t; k_0: zero order constant; k_1: first order constant; k_H: Higuchi constant; k: Korsmeyer-Peppas constant; n: release exponent.

2.7. Study of cytocompatibility

Cytotoxicity tests of AVE-loaded systems were conducted on fibroblast cells using RGB method. Only the formulation F3 was examined at three different concentrations of 10, 100 and 500 ppm. The sample was examined at the Molecule laboratory at HCMC University of Science. Briefly, the cells were incubated in 96-well plates at a density of 10^4 cells/well. After being cultured for 24 hours, the cells were exposed to prepared F3 samples for an additional 24 hours. Afterwards, these wells were treated with cool Trichloroacetic acid at the concentration of 70 v/wt%, followed by straining with Sulforhodamine B 0.2 %. The optical density (OD) values were recorded at 492 nm and 620 nm wavelengths using an ELISA reader. The experiments were repeated 3 times and the average values were expressed as the mean ± standard deviation. The percentage of growth inhibition (% I) was calculated with the following equation [20]:

$$\%\boldsymbol{I} = \left(\mathbf{1} - \frac{\boldsymbol{OD_T}}{\boldsymbol{OD_C}}\right) \times \mathbf{100}\ \% \tag{8}$$

in which, ODT and ODC are the optical density values of test sample and control sample, respectively.

3. RESULTS AND DISCUSSION

3.1. Structural characterizations of AVE-loaded nanoemulsion

To ensure that AVE was loaded onto the F127/P123 scaffold by ultrasonication method, FT-IR measurements were used as the primary test. As illustrated in Fig. 2A, appearance of peaks at wavenumbers: 2969.26 and 2872.42 cm^{-1} correspond to the stretching of C_{sp3}-H bonds; and 1414.9 cm^{-1} represents bending of C_{sp3}-H bonds, characteristic of the unloaded F127/P123 pluronic copolymer. Subsequently, two new peaks unrelated to the structures of F127; P123 or F127/P123 were observed in Fig. 2B. Vibrational bands at wavenumber 3074.65 cm^{-1} correspond to the stretching vibrations of C_{sp2}-H bonds in the aromatic ring of AVE molecule [21, 22]; and that at wavenumber 1759.83 cm^{-1} represents the stretching vibrations of the saturated C=O ester bonds on pluronic – AVE structure [23]. Hence, these experimental data suggest that the ultrasonication - assisted incorporation of AVE into the nanoemulsion (F3) was successful.

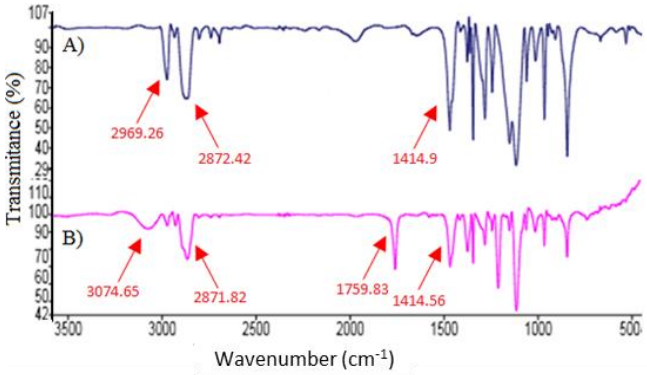

Figure 2. FT-IR spectra of: F127/P123 (1:1 wt/wt %) (A) and F127/P123/AVE (F3) (B) nanoemulsions.

3.2. Physiochemical characterization and stability of AVE-loaded nanoemulsion

Different formulations of pluronic micelles and AVE-loaded nanoemulsions were dispersed in water to concentration of 1000 ppm for DLS measurement. Size distributions of the nanoparticles were recorded and exhibited in Fig. 3. The results showed that pluronic micelles were formed in a smaller size distribution in the range of 20-30 nm (Figs. 3A, 3B) as compared

to that of AVE-loaded nanoemulsions (from 45 to 90 nm), which is dependent on different ratios of pluronic F127. It is worth noting that formulations containing pluronic F127 exhibited a lower size distribution (Figs. 3B; D; E; G). In particular, Fig. 3B exhibited a broad range in size distribution with a PI value of 2.414, indicating that pure F127 nanoemulsion possessed very poor stability. Upon encapsulation of AVE, the stability performance of the pluronic – AVE nanoemulsion improved drastically (Figs. 3D; E; G).

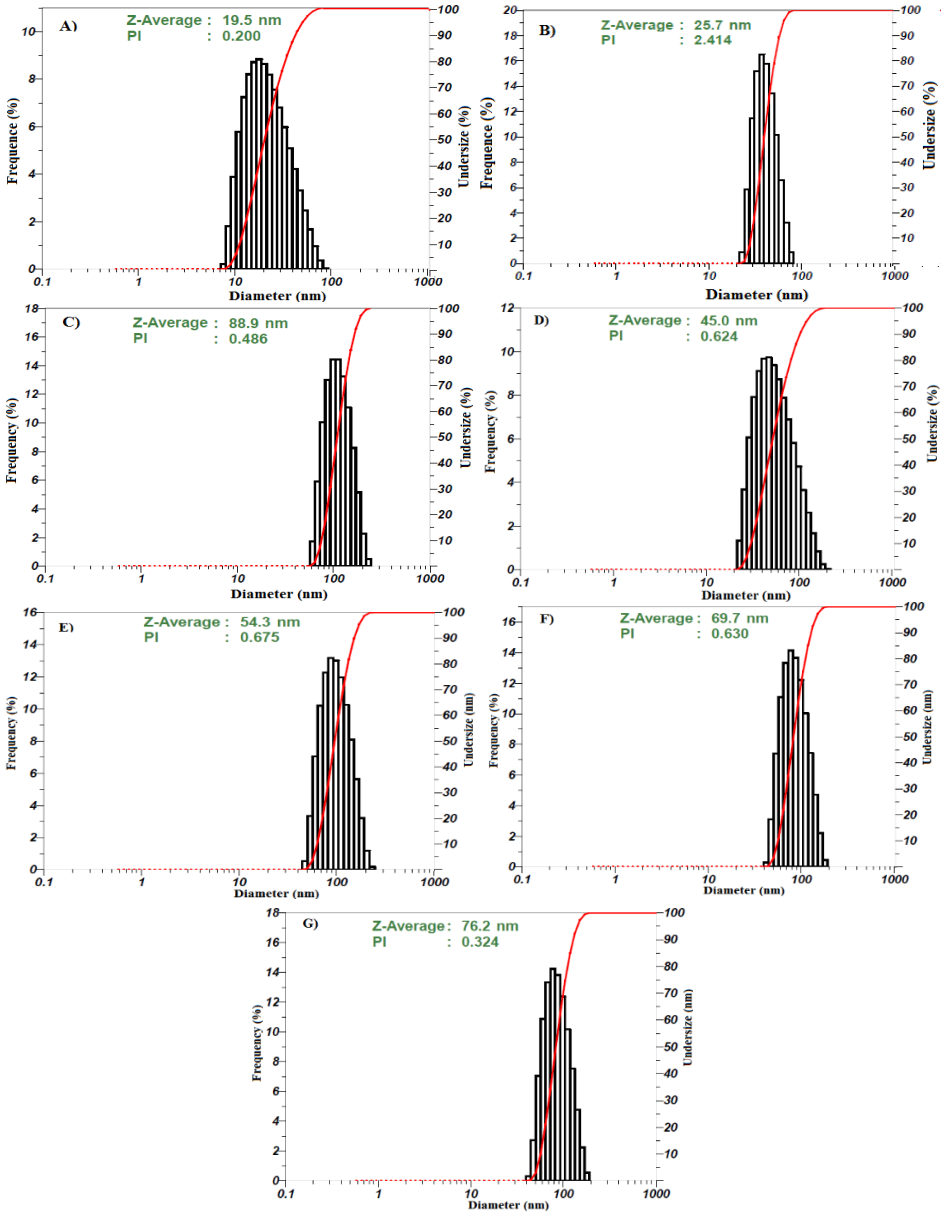

Figure 3. Size distribution of pluronic micelles or its AVE-loaded nanoformulations: P123 (A), F127 (B), F1 (C), F2 (D), F3 (E), F4 (F), F5 (G).

Hence, DLS measurement results suggested that pluronics, especially F127 containing formulations and AVE are compatible for bioactive agents delivery applications. Regarding stability investigation of the nanoemulsions, macroscopic images of the post preparation samples

were recorded after one hour and two storing weeks. The results indicated that the P123-based nanoelmusions (F1; F4) exhibited the lowest stability with a significantly separated phase phenomenon after two storing weeks (red arrow in Figs. 4C, 4F). At the same time, the F127-based nanoelmusions (F2; F5) exhibited a better stability. For the platform based on P123 and F127 mixture (F3), the nanoemulsion is a homogeneous phase after two storing weeks. The difference in performance could be explained by a difference in hydrophilic and hydrophobic balance (HLB) of P123 and F127. Pluronic F127 is a highly-water soluble surfactant with the HLB value of 22. On the other hand, pluronic P123 (HLB = 8) exhibits low solubility at room temperature resulting in a lower payload. However, the higher hydrophilic copolymer derivatives of pluronic P123 could be well-loaded with hydrophobic molecules as compared to the original form [24 - 26]. Moreover, Wei *et al*. indicated that combination of P123 and F127 produced a higher kinetic and steric stabilization of lipid vesicles in aqueous environment than that of P123 micelles alone [27].

In this study, mixture of the P123 and F127 led to a HLB adjustment, which is more appropriate to achieve efficient loading of AVE in the micellar nanoparticle and contributed to stabilizing the nanoemulsion.

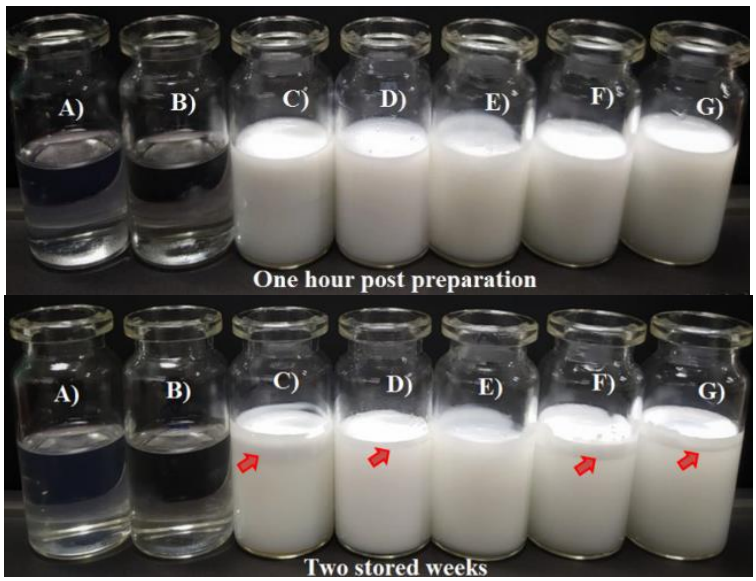

Figure 4. Macroscopic images of micellar pluronic solution and nanoemulsion after one hour post preparation and two storing weeks: P123 (A), F127 (B), F1 (C), F2 (D), F3 (E), F4 (F), F5 (G).

In an additional study, morphology and nanosized emulsion particles of the F3 formulation after two storing weeks were indicated in Fig. 5. The right-hand TEM image is a magnification of that on the left, visualising the morphology of F3 emulsified nanoparticles. The nanoemulsion nanoparticles were formed in a spherical shape ranging from 50 to 70 nm in size with satisfactory uniformity amongst the nanoparticles – which matches with the DLS results for sample F3 obtained above. These nanoparticles are observed to have two distinct regions within its micellar structure: a dark core region consisting of hydrophobic components of the pluronic co-surfactants along with the encapsulated AVE; and the other contrasting lighter region – similar to the colour of the background suggested the hydrophilic groups on the pluronic platforms structure. These results could confirm that the mixed P123 and F123 platform is suitable to load AVE for topical delivery applications.

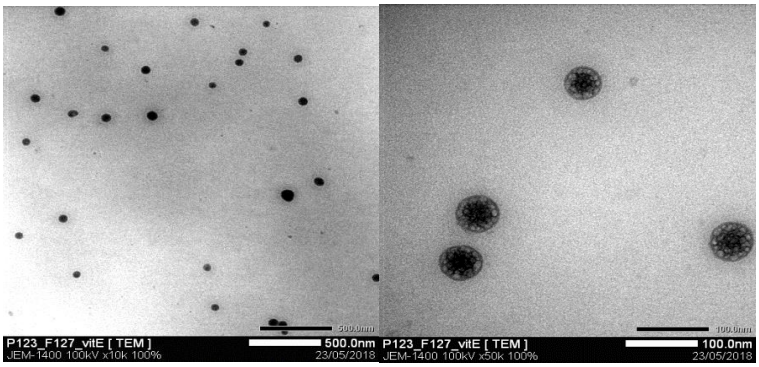

Figure 5. TEM images of the AVE-loaded nanoemulsion (F3 formulation after two storing weeks).

Further experiments after a storage period of six months were also carried out in order to investigate stability performance of the stored F3 sample: additional size distribution DLS measurement in conjunction with microscopic images for morphologic observation. The DLS size distribution measurement results of the F3 sample after being stored for six months are exhibited in Figure 6, nanoparticle size of the sample had increased significantly compared to Fig. 3E. However, the PI value of 0.984 – being below 1.0 suggests that the post 6 months storage F3 sample still possesses acceptable stability despite a sharp rise in size variation.

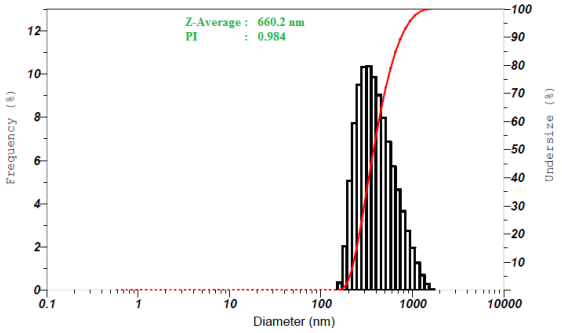

Figure 6. Size distribution of AVE-loaded pluronic nanoformulation F3 after 6 months of storage.

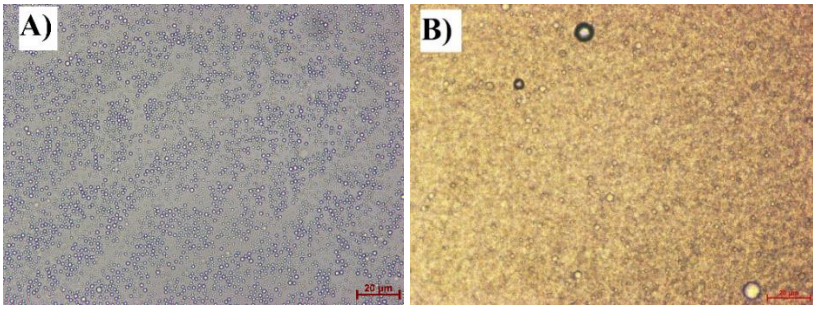

Figure 7. Microscopic images of AVE-loaded F3 sample (A) and after 6 months of storage (B).

Morphological microscopic images of the F3 formulation are shown below in Fig. 7, where the comparison between Figs. 7A. and 7B indicates an accordance with the DLS results in Figure 6 being a significant drop in observable nanoparticles post storage with the accompanying rise in size distribution range. From Fig. 7B, the difference in nanoparticle size can be observed ranging from nanoparticles close in size to the post preparation sample; to larger ones with size similar to the black air – bubbles formed in the image.

3.3. Drug release

Drug load (DL %) and encapsulation (EE %) efficiencies values were determined to be 99.6 ± 0.96 % and 7.97 ± 0.08 %, respectively for F3 encapsulated AVE. The culmulative release curves of AVE encapsulated in F3 nanoemulsion and free AVE are exhibited in Fig. 8 as a function of time. As can be observed, AVE released from F3 nanoemulsion was 2.87 % at conditions simulating a physiological environment within 24 hours. In contrast, the amount of free AVE released from the control sample was 1.28 % in distilled water at 37 ± 1 °C within 24 hours. However – with reference to Fig. 8, the release profile of free AVE exhibits far more fluctuations in release behaviour as compared to that of F3 encapsulated AVE. In details, free AVE being insoluble in water – immediately formed a white precipitate within the membrane as the experiments started. The ethanol solvent used to prepare the free samples diffused out of the membrane as the experiment progressed – dissolving the previously precipitated and promoting further release of AVE, this was confirmed by the sharp increase in released amount recorded. Finally, after the complete diffusion of ethanol, AVE precipitation restarted leading to the essentially flat-line portion of the cumulative release curve of free AVE. In comparison, the release behaviour of F3 encapsulated AVE exhibited far greater stability with only one abnormal point – a decrease in released amount at time-point 7 h. This suggests that at time-point 5 hours, post UV-Vis sample preparation – there was an equilibrium present between the concentration of AVE both within and without the dialysis membrane, hence no further AVE was released between time-points 5 hours and 7 hours. Taking out 1 mL of sample for UV measurement at 7 hours unbalanced the equilibrium and recommenced AVE release, as observed in Fig. 8.

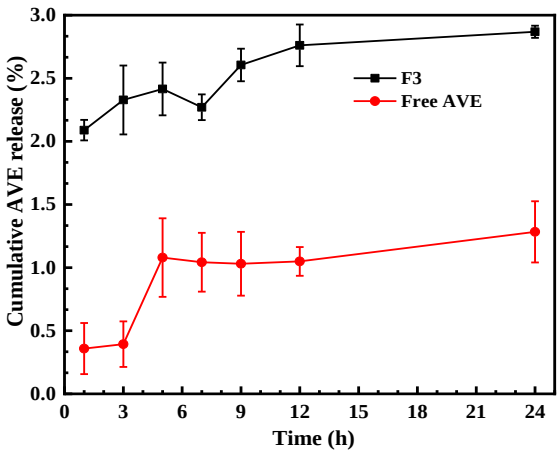

Figure 8. Cumulative release profile of AVE at pH 7.4 and 37 ± 1 °C.

Table 2. AVE kinetic release profile at pH 7.4 and 37 ± 1 °C.

AVE formulation	Mathematical models for drug-release kinetics									Model of release
	Zero order		First order		Higuchi		Power law			
	k_0	R^2	k_1	R^2	k_H	R^2	k	n	R^2	
F3	0.0184	0.8832	0.0673	0.8687	0.0803	0.9252	0.0204	0.1046	0.9200	Fickian

The release results data obtained were fitted into different mathematical models in order to determine the mechanism of AVE release from F3 nanoemulsion. The regression coefficients

(R^2) and release kinetic constants (k), respective of each model used were compiled and exhibited in Table 2, which suggest that EVA release data showed good correlation with Higuchi model kinetics. The release exponent was determined to be 0.1046 and agreed with a Fickian mode. Free EVA didn't give the kinetic release profile due to its precipitation in dialysis membrane.

3.4. Cytocompatibility of AVE-loaded nanoemulsion

Table 3. In vivo cytotoxicity of AVE-loaded nanoemulsion.

Concentration (ppm)	The percentage of growth inhibition (%I)			
	$\%Replicate_1$	$\%Replicate_2$	$\%Replicate_3$	Mean $\pm$ SD
500	-0.81	1.84	2.53	1.19 $\pm$ 1.76
100	-2.44	-4.15	1.44	-1.71 $\pm$ 2.87
10	-2.44	-5.99	2.17	-2.09 $\pm$ 4.09

To assess the cytocompatibility of AVE-loaded nanoemulsion, *in vivo* cytotoxicity was evaluated using different fibroblast cell lines (Hs68; ATCCCRL-1635). The results were illustrated in Table 3 indicating that AVE-loaded nanoemulsion possessed a great cytocompatibility upon the investigated concentration of 500 ppm which could be a potent ingredient in producing skincare products.

4. CONCLUSIONS

AVE-loaded nanoemulsion was successfully fabricated via the ultrasonic-assisted method with size distribution ranging from 50 to 90 nm. Combination of these two kinds of pluronic surfactants produced the highly stable nanosized emulsion particles. The AVE-loaded nanoemulsion exhibited a sustainably release behavior and satisfactory cytocompatibility that may facilitate easier crossing of the skin barrier to display antioxidative and photoprotective properties which could pave the way to applying the method or materials in the development of commercial skincare products.

Acknowledgements. This research is funded by Vietnam National Foundation for Science and Technology Development (NAFOSTED) under grant number 104.02-2019.53.

CRediT authorship contribution statement. Khanh Hoang Vuong, Dang Le Hang and Doan Tran Buu Tai: Methodology, Investigation, Funding acquisition. Tuong Van Vo Le and Tan Phuoc Ton: Formal analysis. Nguyen Dinh Trung: Formal analysis, Supervision. Ngoc Quyen Tran: Formal analysis. Supervision.

Declaration of competing interest. The authors declare that they have no known competing financial interests or personal relationships that could have appeared to influence the work reported in this paper.

REFERENCES

1. Grebenstein N., Schumacher M., Graeve L., and Frank J. - α-Tocopherol transfer protein is not required for the discrimination against γ-tocopherol in vivo but protects it from side-chain degradation in vitro, Mol. Nutr. Food. Res. **58** (5) (2014) 1052-1060. doi: 10.1002/mnfr.201300756.
2. Zingg J. M. - Vitamin E: regulatory role on signal transduction, IUBMB life **71** (4) (2019) 456-478. doi: 10.1002/iub.1986.

3. Lewis E. D., Meydani S. N., and Wu D. - Regulatory role of vitamin E in the immune system and inflammation, IUBMB life **71** (4) (2019) 487-494. doi: 10.1002/iub.1976.
4. Regner-Nelke L., Nelke C., Schroeter C. B., Dziewas R., Warnecke T., Ruck T., and Meuth S. G. - Enjoy carefully: the multifaceted role of vitamin E in neuro-nutrition, Int J Mol Sci. **22** (18) (2021) 10087. doi: 10.3390/ijms221810087.
5. Ungurianu A., Zanfirescu A., Niţulescu G., and Margină D. - Vitamin E beyond its antioxidant label, Antioxidants **10** (5) (2021) 634. doi: 10.3390/antiox10050634.
6. Vinardell M. P. and Mitjans M. - Nanocarriers for delivery of antioxidants on the skin, Cosmetics **2** (4) (2015) 342-354. doi: 10.3390/cosmetics2040342.
7. Thiele J. J., Hsieh S. N., and Ekanayake-Mudiyanselage S. - Vitamin E: critical review of its current use in cosmetic and clinical dermatology, Dermatol Surg. **31** (2005) 805-813. doi: 10.1111/j.1524-4725.2005.31724.
8. Trombino S., Cassano R., Muzzalupo R., Pingitore A., Cione E., and Picci N. - Stearyl ferulate-based solid lipid nanoparticles for the encapsulation and stabilization of β-carotene and α-tocopherol, Colloids Surf B Biointerfaces **72** (2) (2009) 181-187. doi: 10.1016/j.colsurfb.2009.03.032.
9. de Carvalho S. M., Noronha C. M., Floriani C. L., Lino R. C., Rocha G., Bellettini I. C., Ogliari P. J., and Barreto P. L. M. - Optimization of α-tocopherol loaded solid lipid nanoparticles by central composite design, Industrial Crops and Products **49** (2013) 278-285. doi: 10.1016/j.indcrop.2013.04.054.
10. Doan P., Nhi T. T. Y., Nguyen D. T., Nguyen B. T., Nguyen T. P., and Tran N. Q. - Multifunctional injectable pluronic-cystamine-alginate-based hydrogel as a novel cellular delivery system towards tissue regeneration, Int. J. Biol. Macromol. **185** (2021) 592-603. doi: 10.1016/j.ijbiomac.2021.06.183.
11. Ganguly R., Kumar S., Tripathi A., Basu M., Verma G., Sarma H., Chaudhari D., Aswal V., and Melo J. - Structural and therapeutic properties of Pluronic® P123/F127 micellar systems and their modulation by salt and essential oil, Journal of Molecular Liquids **310** (2020) 113231. doi: 10.1016/j.molliq.2020.113231..
12. Basudkar V., Gharat S. A., Momin M. M., and Shringarpure M. - A review of anti-aging nanoformulations: recent developments in excipients for nanocosmeceuticals and regulatory guidelines, Critical Reviews™ in Therapeutic Drug Carrier Systems **39** (3) (2022).
13. Pandey A. S., Bawiskar D., and Wagh V. - Nanocosmetics and Skin Health: A Comprehensive Review of Nanomaterials in Cosmetic Formulations, Cureus **16** (1) (2024). doi: 10.7759/cureus.52754.
14. Neunert G., Szwengiel A., Walejko P., Witkowski S., and Polewski K. - Photostability of alpha-tocopherol ester derivatives in solutions and liposomes. Spectroscopic and LC–MS studies, Journal of Photochemistry and Photobiology B: Biology **160** (2016) 121-127. doi: 10.1016/j.jphotobiol.2016.03.032.
15. Nguyen D. T., Dinh V. T., Dang L. H., Nguyen D. N., Giang B. L., Nguyen C. T., Nguyen T. B. T., Thu L. V. and Tran N. Q. - Dual interactions of amphiphilic gelatin copolymer and nanocurcumin improving the delivery efficiency of the nanogels, Polymers **11** (5) (2019) 814. doi: 10.3390/polym11050814
16. Nguyen N. T., Bui Q. A., Nguyen H. H. N., Nguyen T. T., Ly K. L., Tran H. L. B., Doan V. N., Nhi T. T. Y., Nguyen N. H., and Nguyen N. H. - Curcuminoid co-loading platinum

heparin-poloxamer P403 Nanogel increasing effectiveness in antitumor activity, Gels **8** (1) (2022) 59. doi: 10.3390/gels8010059.

17. Rajaei M., Rashedi H., Yazdian F., Navaei-Nigjeh M., Rahdar A. and Díez-Pascual A. M. - Chitosan/agarose/graphene oxide nanohydrogel as drug delivery system of 5-fluorouracil in breast cancer therapy, Journal of Drug Delivery Science and Technology **82** (2023) 104307. doi: 10.1016/j.jddst.2023.104307.
18. Li P., Dai Y. N., Zhang J. P., Wang A. Q., and Wei Q. - Chitosan-alginate nanoparticles as a novel drug delivery system for nifedipine, International journal of biomedical science: IJBS **4** (3) (2008) 221.
19. Upputuri R. T. P. and Mandal A. K. A. - Mathematical modeling and release kinetics of green tea polyphenols released from casein nanoparticles, Iranian Journal of Pharmaceutical Research: IJPR **18** (3) (2019) 1137.
20. Cheng C. C., Lee D. J., and Chen J. K. - Self-assembled supramolecular polymers with tailorable properties that enhance cell attachment and proliferation, Acta Biomaterialia **50** (2017) 476-483. doi: 10.1016/j.actbio.2016.12.031.
21. Anirudhan T., Varghese S., and Manjusha V. - Hyaluronic acid coated Pluronic F127/Pluronic P123 mixed micelle for targeted delivery of Paclitaxel and Curcumin, Int J Biol Macromol. **192** (2021) 950-957. doi: 10.1016/j.ijbiomac.2021.10.061.
22. Liu X., Li Y., He J., Zhao T., Chen C., Gu H., and Wang X. - Paclitaxel-loaded pluronic F127/P123 silica nanocapsules with surface conjugated rhTRAIL for targeted cancer therapy, RSC Advances **7** (48) (2017) 30250-30261. doi: 10.1039/c7ra04503d.
23. Shah F., Sarheed O., and Usman S. - Development and evaluation of a cream containing solid lipid nanoparticles loaded with Vitamin E, Pak J Pharm Sci. **34** (6) (2021).
24. Nguyen V. T., Nguyen T. H., Dang L. H., Vu-Quang H., and Tran N. Q. - Folate-Conjugated Chitosan- Pluronic P123 Nanogels: Synthesis and Characterizations towards Dual Drug Delivery, Journal of Nanomaterials **2019** (1) (2019) 1067821. doi: 10.1155/2019/1067821.
25. Van Thoai D., Nguyen D. T., Dang L. H., Nguyen N. H., Nguyen V. T., Doan P., Nguyen B. T., Thu L. V., Tung N. N., and Quyen T. N. - Lipophilic effect of various pluronic-grafted gelatin copolymers on the quercetin delivery efficiency in these self-assembly nanogels, J. Polym. Res. **27** (2020) 1-12. doi: 10.1007/s10965-020-02216-z.
26. Nguyen T. T. C., Nguyen C. K., Nguyen T. H., and Tran N. Q. - Highly lipophilic pluronics-conjugated polyamidoamine dendrimer nanocarriers as potential delivery system for hydrophobic drugs, Materials Science and Engineering: C **70** (2017) 992-999. doi:10.1016/j.msec.2016.03.073.
27. Wei Z., Hao J., Yuan S., Li Y., Juan W., Sha X., and Fang X. - Paclitaxel-loaded Pluronic P123/F127 mixed polymeric micelles: formulation, optimization and in vitro characterization, International Journal of Pharmaceutics **376** (1-2) (2009) 176-185. doi: 10.1016/j.ijpharm.2009.04.030.